



## ORIGINAL ARTICLE

# Shape-directing role of cetyltrimethylammonium bromide on the morphology of extracellular synthesis of silver nanoparticles



Shael Ahmed Al-Thabaiti <sup>a</sup>, Abdullah Yousif Obaid <sup>a</sup>, Shokit Hussain <sup>b</sup>,  
Zaheer Khan <sup>a,\*</sup>

<sup>a</sup> Department of Chemistry, Faculty of Science, King Abdulaziz University, P.O. Box 80203, Jeddah 21589, Saudi Arabia

<sup>b</sup> Department of Chemistry, Jamia Millia Islamia (Central University), New Delhi 110025, India

Received 19 April 2013; accepted 15 November 2014

Available online 29 November 2014

## KEYWORDS

Silver nano-disks;  
Morphology;  
CTAB;  
Kinetics

**Abstract** *Oriental plane* leaf extracts were used as a reducing-, stabilizing- and capping-agent for the preparation of silver nanoparticles (AgNPs) for the first time. The size, shape, size distribution and optical properties strongly depend on the experimental conditions, absence, and presence of shape-directing cetyltrimethylammonium bromide (CTAB). UV–vis spectroscopy, transmission electron microscopy and selected electron diffraction ring patterns were used to determine the morphology of resulting AgNPs at different time intervals. The spectra showed a surface Plasmon resonance (SPR) peak at 450 nm which is the characteristic of spherical AgNPs (diameter ranging from 10 to 30 nm). The peak shifted to shorter wavelength (blue shift) from 450 to 425 nm and sharpness of the peak also decreases in the presence of CTAB which might be due to the capping action of CTAB. A layer of ca. 3 nm around a group of the AgNPs in which the inner layer is bound to the AgNPs surface via the active groups of the extract has been observed.

© 2014 The Authors. Production and hosting by Elsevier B.V. on behalf of King Saud University. This is an open access article under the CC BY-NC-ND license (<http://creativecommons.org/licenses/by-nc-nd/3.0/>).

## 1. Introduction

The use of different surfactants (normal and Gemini) as stabilizers and/or capping agents has been the subject of various

researchers for two decades (Mulvaney, 1996; Chen et al., 2003). Morphology of gold and silver AgNPs (cubes, hollow structures, disks, prisms, sheets/plates, wires/rods, multi-branched and/or multi-pods) strongly depends on the nature and presence of stabilizer (Bakshi, 2009). Bakshi et al. (2008) used the seed-mediated approach to synthesize gold nanoparticles by using twin tail alkylammonium cationic Gemini surfactant such as hexamethylene-1,6-bis(dodecyldimethylammonium bromide) (12-6-12) and didodecyldimethylammonium bromide (12-0-12) as capping agents in aqueous phase. Spherical and nanorods were obtained in the presence of 12-6-12 while no anisotropic growth was observed with 12-0-12 as a

\* Corresponding author.

E-mail address: [drkhanchem@yahoo.co.in](mailto:drkhanchem@yahoo.co.in) (Z. Khan).

Peer review under responsibility of King Saud University.



Production and hosting by Elsevier

capping agent. Salavati-Niasari and his co-workers synthesized copper indium sulfide nanocrystals, CdSe/CdS core/shell nanoparticles by using the micro wave, ultrasonic, and precipitation methods (Sabet et al., 2013; Amiri et al., 2013, 2014a). They also investigated the photo catalyst activity of CdSe/CdS core/shell nanoparticles (Amiri et al., 2014a) and application of copper indium sulfide nanoparticles for solar cell (Amiri et al., 2014b). Mono-dispersed lanthanum hydroxide nanoparticles and nanorods, and bismuth sulfide nanorods were reported by Salavati-Niasari et al. (2012, 2013). The literature is replete with the investigations of the use of different stabilizers during the synthesis and characterization of advanced nanomaterials of various metals. But the use of shape-directing cetyltrimethylammonium bromide in the similar investigations involving plants leaves and seeds as reducing agents has been neglected (Pileni, 1993; Khan et al., 2012a,b). Various natural reducing agents such as medicinal plants, leaves, flowers, seeds and their bark are used as an alternate source of the toxic reductants (Shiv Shankar et al., 2004; Sharma et al., 2007; Al-Thabaiti et al., 2008). Reduction ability of natural reducing agents strongly depends on the reduction potentials of reducing agents.

The leaves of *Oriental plane* are used for the treatment of astringent, dysentery, heal wounds, chilblains and ophthalmia. A large number of molecules such as platanin, tannin, allantoin, glyoxylic acid, phlobaphene, mannitol, platanolic acid and platanol are the bioactive constituents of chinar leaves. Recently, we have reported the use of various reducing agents (citric acid, ascorbic acid, sugars and amino acids) in the synthesis of advanced AgNPs in the presence of shape-directing CTAB (Al-Thabaiti et al., 2008; Khan et al., 2012; Hussain and Khan, 2014). In this paper, we describe a one-pot chemical reduction method for the synthesis of AgNPs using aqueous leaf extracts of *Oriental plane* (deciduous tree of the Platanaceae family). To the best of our knowledge, this is the first ever report on *Oriental plane*-assisted extracellular green synthesis of advanced AgNPs in the absence and presence of shape-directing CTAB cationic surfactant. The method is simple, clean and requires only the extract and AgNO<sub>3</sub>. In addition, this method has an advantage in higher scale production of AgNPs over the various methods reported in the literature.

## 2. Experimental

### 2.1. Chemicals

Deionized double distilled (first time from alkaline KMnO<sub>4</sub>), CO<sub>2</sub> and O<sub>2</sub> free water was used as the solvent. All glassware was washed with aqua regia (3:1 HCl and HNO<sub>3</sub>), rinsed with water, and dried prior to use. Silver nitrate (AgNO<sub>3</sub>, oxidant, Merck India, 99.99%), and CTAB (99%, stabilizer, Fluka) were used without further purification. Fresh chinnar leaves collected from the Srinagar, Jammu and Kashmir, India, were perfectly washed, chopped into small pieces and added to a Borosil conical flask containing 250 ml double distilled deionized water. The reaction mixture was kept on a boiling water bath for 30 min, cooled and filtered through What-man filter paper no. 40. The perfect transparent clear filtrate contains only soluble organic moieties of the chinnar leaves stored in an amber glass bottle. This resulting aqueous solution is used for the reduction of Ag<sup>+</sup> ions to the Ag<sup>0</sup>.

### 2.2. Preparation and characterization of AgNPs

In a typical experiment, fresh solution of AgNO<sub>3</sub> was added to the reaction mixture containing required amounts of leaf extracts and kept at room temperature for the reduction process. As the reaction time increases, appearance of pale-yellow is observed indicating the formation of AgNPs (Hussain and Khan, 2014; Zhang et al., 2004). Shimadzu UV-vis spectrophotometer; model UV-1800, Japan and transmission electron microscope (Hitachi 7600 with an accelerating voltage of 120 kV) were used to record the spectra and determine the morphology (size, shape and the size distribution) of resulting AgNPs, respectively. Selected area electron diffraction (SADE) data were also recorded. XRD patterns of the samples were recorded using Ni-filtered Cu K $\alpha$  radiation ( $\lambda = 1.54056 \text{ \AA}$ ) of a Rigaku X-ray diffractometer operating at 40 kV and 150 mA at a scanning rate of 0.02<sup>o</sup> per step in the 2 $\theta$  range of 10<sup>o</sup>  $\leq$  20<sup>o</sup>  $\theta$   $\leq$  80<sup>o</sup>.

## 3. Results and discussion

### 3.1. Visual observations and UV-vis spectra

It has been established that metallic silver in nano and/or colloidal state gives different colors in aqueous solutions due to the excitation of electron from the valence bond to conduction bond (Mulvaney, 1996). In the first set of experiments, observation shows that the required amounts of leaf extracts and aqueous AgNO<sub>3</sub> solution were colorless. As the reaction time increases, the color of the reaction mixture changed from pale-yellow, pink-yellow, light brown, and wine-red to dark brown. Optical images of leaf extracts, AgNO<sub>3</sub> and different colors formed after the reduction of Ag<sup>+</sup> ions with extracts are given in Fig. 1. Appearance of different colors at different time intervals (from initial to final stage) indicates that the morphology of AgNPs (shape, size and the size distribution) alters with the reaction time. The appearance and/or change of color strongly depend on the reaction conditions and [extract] and/or [Ag<sup>+</sup>] which is due to regular aggregation. The position and shape of the SRP absorption depend on the particle size, shape, and dielectric constant of the surrounding medium and surface-adsorbed species. The broadening of the absorption band with [Ag<sup>+</sup>] indicates that initially reduced AgNP grows to form larger particles, and finally, Ag<sup>+</sup> acts as a shape-directing agent. The shift of the plasmon peak to higher wavelengths may happen due to various reasons (Zhang et al., 2004). The spectra of the synthesized AgNPs are also recorded at different time intervals for the variation of leaf extracts (Fig. 2). The surface Plasmon resonance (SPR) peak observed at 450 nm confirms the influence of aqueous chinnar leaf extracts in reducing Ag<sup>+</sup> ions to Ag<sup>0</sup> (formation of AgNPs from aqueous AgNO<sub>3</sub> solution). Absorbance intensity of broad SPR band increases steadily as a function of reaction time suggesting the anisotropic growth of AgNPs. A weak absorbance peak was observed at 450 nm with 1.0 cm<sup>3</sup> of extracts after 5 min. Interestingly, the position of the maximum absorption was shifted to a shorter wavelength (from 450 to 425 nm; blue shift). The red- and/or blue-shifting of the absorption band with [extract] indicate that initially small AgNPs grow to form larger particles and finally extracts act as shape-directing agents (Linnert et al., 1990). The blue-shifting is probably due to the interparticle interaction in the

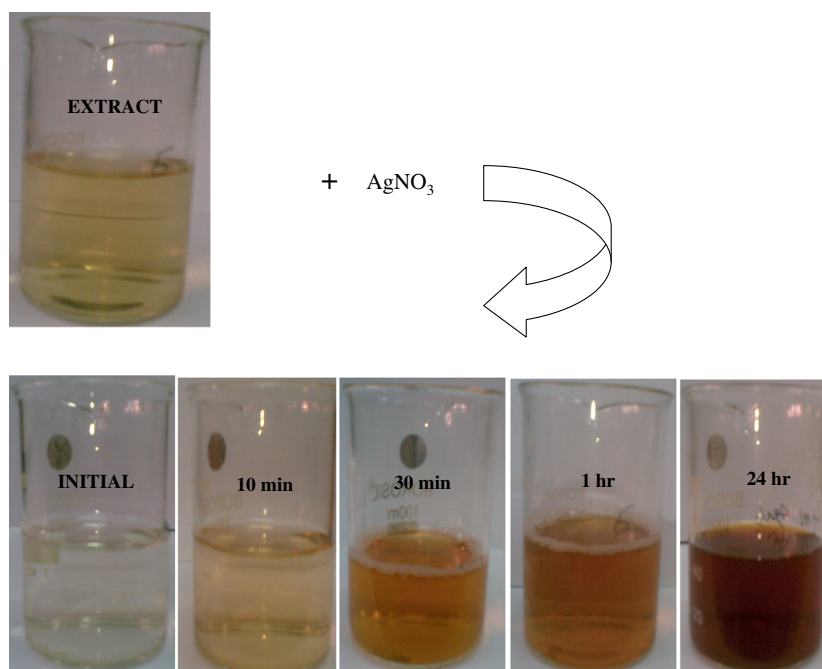


**Figure 1** Optical images of AgNPs at different time intervals. *Reaction conditions:*  $[Ag^+] = 4.0 \times 10^{-4} \text{ mol dm}^{-3}$ ,  $[\text{extract}] = 5.0 \text{ cm}^3$ , temperature = 30 °C.

high-concentrated water soluble AgNPs. Interestingly, our spectra do not show a tail extending into the red (Fig. 2), indicating that the resulting AgNPs have significant aggregation. The broadness of the peak indicates the wide size distribution of the nanoparticles in the biomolecules constituents of leaf extracts (Song and Kim, 2009). Shape and nature of the spectra provide an understanding about the morphology of noble metal nanoparticles. The peak intensity increases with time which might be due to the formation of tiny AgNPs which simultaneously converted into the bigger AgNPs with reaction time (Fig. 3). In addition to a sharp peak at 425 nm, a weak shoulder also developed at 450 which might be due to the anisotropic growth of AgNPs. The blue shift might be due to the multiplasmon excitation of faceted and anisotropic AgNPs (Jin et al., 2001) and the peak at 450 nm depends on the sharpness of the corner of silver triangles (nanodisks; Fig. 2). The nanoplates (nanodisks) could be formed by the dissolution of the corner atoms of truncated triangular nanoplates.

### 3.2. Kinetic and mechanism

The reaction–time curves show that the  $Ag^+$  ion reduction into  $Ag^0$  occurs very rapidly and more than 90% of the reduction of  $Ag^+$  ions will be completed in 10 min. From 10 to 30 min, the reaction stops as the intensity of the reaction shows almost a parallel line with  $x$ -axis with respect to time (Fig. 3). No appreciable change in absorbance was noticed after 10 min for all the  $[Ag^+]$  used in the entire study, confirming the complete reduction of  $Ag^+$  ions to AgNPs. The sigmoidal shape of the reaction–time curves clearly suggests that autocatalysis was involved in the path of AgNPs formation (Mehta et al., 2010). Surprisingly, formation of transparent pale yellow color silver sol was not observed at lower  $[Ag^+]$  ( $\leq 2.0 \times 10^{-4} \text{ mol dm}^{-3}$ ) whereas, yellowish-white precipitate was also formed at higher

$[Ag^+]$ . Therefore, it can now be stated confidently that the formation of AgNPs is not directly proportional to the  $[Ag^+]$ ; small  $[Ag^+]$  being enough to initiate the formation of metal nucleation center which acts as a catalyst for the reduction of other  $Ag^+$  present in the reaction mixture. Hydroxy groups of reducing sugars and/or platanolic acid reduce  $Ag^+$  into  $Ag^0$  (Eq. (1); rate-determining step, rds). The neutral atom  $Ag^0$  reacts with  $Ag^+$  to form the relatively stabilized  $Ag_2^+$  clusters as shown in Eq. (3).  $Ag_2^+$  clusters dimerize to yield  $Ag_4^{2+}$  (yellow-color silver sol; stable species for a long time in the presence of a polyanion even under air and growth stops at the stage of this species (Eq. (4)) (Henglein, 1993). The intervention of free radical was detected by adding acrylonitrile as a scavenger, the formation of white precipitate appeared slowly as the reaction proceeded indicating in situ generation of free radicals. Control experiments with  $Ag^+$  ions and leaf extracts did not show formation of a precipitate. On the basis of above Section 3, Scheme 1 is proposed as a mechanism for the formation of AgNPs by the bioactive constituents of chinnar leaf extracts.

### 3.3. Shape-directing effect of CTAB

Micelles, dynamic aggregates can alter morphology and other surface optical properties to different extents depending up on their nature of head group, type of counter-ions and length of hydrophobic tail (Pal et al., 1997). Surfactants are the amphiphilic molecules, which create highly anisotropic interfacial regions lining the boundary formed by the highly polar aqueous and nonpolar hydrocarbon regions. Micelles affect reaction rates by incorporating the substrate into the micellar aggregate, rather than by changing the solvent properties of water. The hydrophobic, electrostatic and hydrogen bonding are the main factors involved in the rate enhancement of a

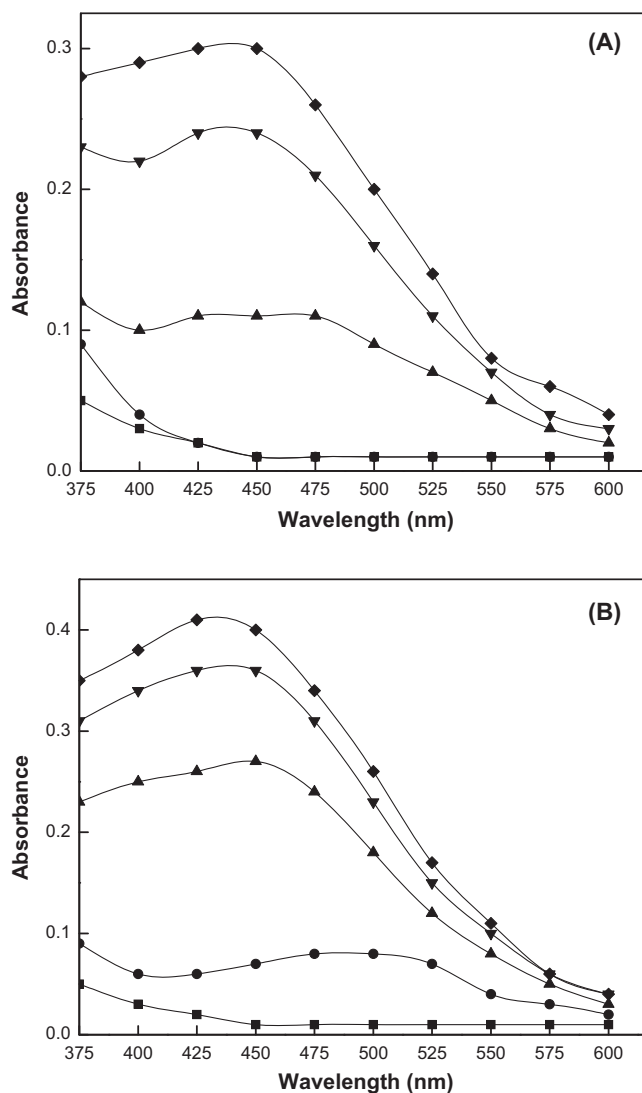


**Figure 2** Absorption spectra of extract (■) and AgNPs. *Reaction conditions:* [CTAB] = 0.0 mol dm<sup>-3</sup>; [extract] = 5.0 cm<sup>3</sup>; [Ag<sup>+</sup>] = 4.0 × 10<sup>-4</sup> (A) and 8.0 × 10<sup>-4</sup> mol dm<sup>-3</sup> (B); time = 5 (●), 10 (▲), 20 (▼) and 30 min (◆).

bimolecular reaction. Fig. 4 clearly demonstrates the CTAB catalytic effect not only above but even below the CMC (i.e., micellar as well as pre-micellar catalyses are observed). In order to get insights into the sub- and post-micellar roles of shape-directing CTAB, a series of experiments were performed at two different [CTAB] i.e., 4.0 × 10<sup>-4</sup> and 8.0 × 10<sup>-4</sup> mol dm<sup>-3</sup> at fixed concentrations of other reagents. The observed results are summarized in Fig. 4 as absorbance–wavelength profiles. The intensity of the SRP band was increased rapidly with time. However, the position of the maximum absorption was shifted to a shorter wavelength with the variation of reaction-time, indicating that much smaller AgNPs were generated in the presence of CTAB. The peak at short wavelength may be attributed to the out-of plane quadrupole. The effect of [CTAB] on the morphology and reaction-time curves can be rationalized by considering the distribution, incorporation, and/or solubilization of the reactants (Ag<sup>+</sup> ions and active constituents of aqueous leaf extracts) among the different

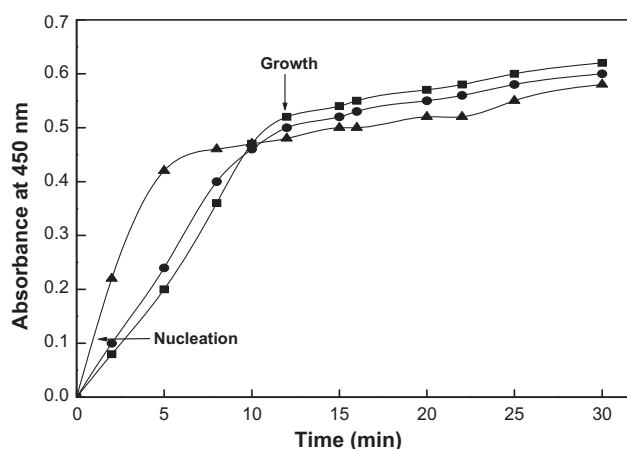
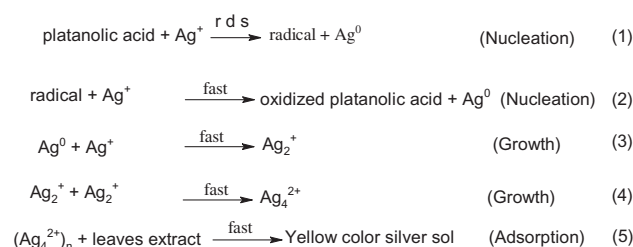


**Figure 3** Effect of [extract] on the nucleation and growth of AgNPs. *Reaction conditions:* [Ag<sup>+</sup>] = 16.0 × 10<sup>-4</sup> mol dm<sup>-3</sup>; [CTAB] = 0.0 × 10<sup>-4</sup> mol dm<sup>-3</sup>; [extract] = 5.0 (▲), 10.0 (●) and 15.0 cm<sup>3</sup> (■).



**Scheme 1** Reduction of Ag<sup>+</sup> ions into the metallic silver.

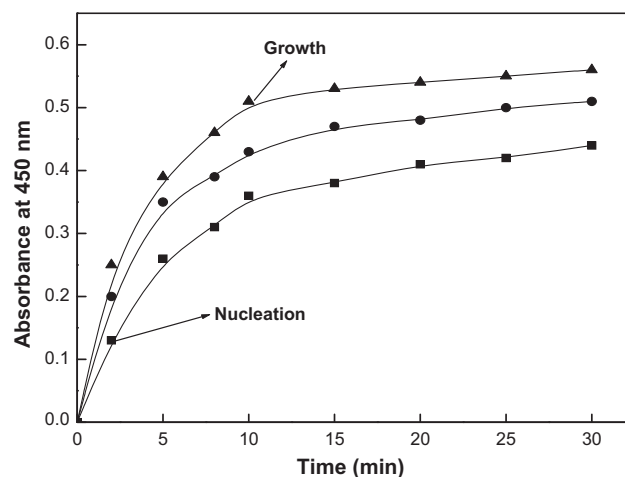
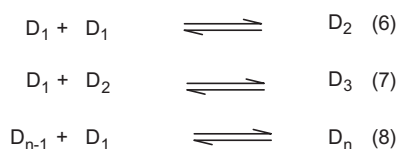


**Figure 4** Effect of [CTAB] on the nucleation and growth of AgNPs. *Reaction conditions:* [Ag<sup>+</sup>] = 16.0 × 10<sup>-4</sup> mol dm<sup>-3</sup>; [extract] = 5.0 cm<sup>3</sup>; [CTAB] = 4.0 (▲), 8.0 (●) and 12.0 × 10<sup>-4</sup> mol dm<sup>-3</sup> (■).

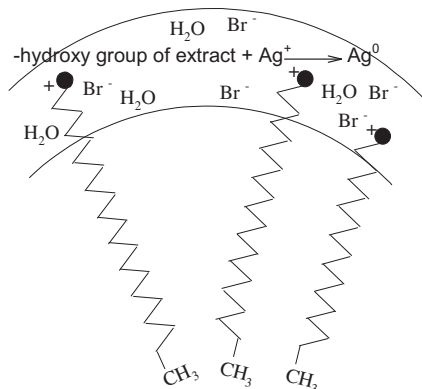
pseudo phases present in the reaction medium. Accordingly to the multiple equilibrium model, the distribution of surfactant ( $D_1$ ) between various states of aggregation is controlled by a series of dynamic association–dissociation equilibria: (Scheme 2).



**Scheme 2** Association of reactants with different aggregates of CTAB.

The shape-directing role of CTAB can be sought in the fact that small aggregates of the CTAB exist below the CMC; these small submicellar aggregates can interact physically with the reactants forming active entities. Bakshi and his co-workers (Bakshi, 2010), used different surfactants, anionic, cationic and Gemini to the synthesis of multi branched advanced Ag- and Au-NPs and reported these stabilizer(s) acted as a shape-directing agents. In the present system, reactions occur between the micellar solubilized constituents of extracts and silver ions present in the junctural region of palisade – Stern layers. Micellization increases the reaction rate because on micellization counterions can be attracted or repelled more effectively. The frequency of molecular collisions increases as a consequence of the close association of the two reacting species at the micellar interface. In micelle-mediated reactions, it is not possible to precisely locate the exact site of the reaction but, at least, localization of the reactants can be considered (micellar surfaces are water-rich and do not provide a uniform reaction medium because a micelle is a porous cluster with a rough surface and deep-water-filled cavities). A possible arrangement (although highly schematic) could be that as shown in Scheme 3.

Cierpiszewski et al. (1996) have advised to avoid the use of even buffer solutions to maintain pH of micellar solutions (control of pH and of ionic strength is not as straightforward in micellar solutions as in ordinary solvents). CTAB solution became turbid in the presence of HClO<sub>4</sub>. Anions were found to be strongly adsorbed on the AgNPs (adsorption of nucleophile on the particle surface increases the Fermi level of silver particles). It was also observed that the stability of colloidal and nano size metal particles depend strongly on the pH of the reaction medium (Khan et al., 2004). Therefore, no mineral acid was used to maintain the pH constant. Silver sol solution



**Scheme 3** Probable reaction site for the reduction of silver ions by the hydroxyl group.

undergoes acid hydrolysis or is unstable in aqueous solutions of  $[H^+] > 1.0 \times 10^{-3} \text{ mol dm}^{-3}$ . In the redox reactions of  $Ag^+$  ions with organic reductants, the medium of the reaction mixture plays an important role. The formation of long-lived oligomeric silver clusters has been observed only in the neutral–acidic solution. On the other hand, these clusters destabilize in strongly acidic medium and form unreactive large silver particles. Therefore, it should be emphasized here that reactions were studied without adding acidifying agents (HClO<sub>4</sub> and H<sub>2</sub>SO<sub>4</sub>). However, a series of experiments were also performed in order to see any change in the macroscopic pH of the working solution in the presence of [CTAB] and/or extracts. The pH value was found to be nearly constant with increasing [CTAB] and [extract] (pH = 5.0, 5.2, 5.3, 5.4 and 5.2 for [CTAB] = 8.0, 9.0, 10.0, 12.0 and  $16.0 \times 10^{-4} \text{ mol dm}^{-3}$ , respectively). It is not surprising because ionic micelles show a marked difference in the effective local pH to exist at its micellar surface over that in bulk aqueous solvent. In a typical experiment, 5.0 cm<sup>3</sup> (0.01 mol dm<sup>3</sup>) NaCl was added to a reaction mixture containing the extract (10.0 cm<sup>3</sup>) + AgNO<sub>3</sub> (10.0 cm<sup>3</sup> of 0.01 mol dm<sup>3</sup>) + CTAB 5.0 cm<sup>3</sup> of (0.01 mol dm<sup>3</sup>) after 40 min the absorbance of the perfect transparent yellow orange color silver sol became constant (Fig. 3). We did not observe the white precipitate and/or turbidity of AgCl indicating the complete reduction of  $Ag^+$  ions to  $Ag^0$ . The particles were separated from the solutions by centrifugation at 10,000 rpm for 15 min. They were then re-suspended in water and the centrifugation was repeated twice so as to remove impurities. The yield was found to be ca. 90%.

### 3.4. TEM images and SAED patterns

TEM images and SAED ring patterns of AgNPs are summarized in Fig. 5. These images show that CTAB has a marked effect on the morphology. Inspection of TEM images clearly suggests that the AgNPs were mostly truncated triangular nanoplates/nano-disks, irregular and poly-dispersed with a large number of quantum dots of 3 nm (Fig. 5A). The TEM analyses corroborate well with the results drawn from the corresponding reaction–time curves. In the presence of CTAB, the interactions and solubilization of reducing molecules occur with the positive head group of CTAB. The AgNPs are also adsorbed and/or bound with the CTAB due to the electrostatic and van der Waals forces, which in turn, altered the morphology drastically and the number of spherical shaped AgNPs was also increased (Fig. 5). TEM micrographs clearly indicate the presence of coatings surrounding the AgNPs which might be due to the terpenoids and/or reducing sugars present in leaf extracts which acted as reducing- and capping-agents (Jin et al., 2001). Fig. 5A shows the TEM images of silver nanodisks in this study (length 96.63 nm, width 10 nm). On careful observation of TEM images, a thin shell (layer = 3 nm) of extract constituents covered on the groups of various AgNPs is seen. The capping is prominent on each particle and the same may also be responsible for interparticle binding. Each silver nanodisk is a group of several truncated triangular nanoplates (indicated by arrow in Fig. 5A: large fraction of triangles having round corners). The typical selected-area diffraction pattern is shown in Fig. 5B. The ring patterns are consistent with the plane families {110}, {111}, {200},

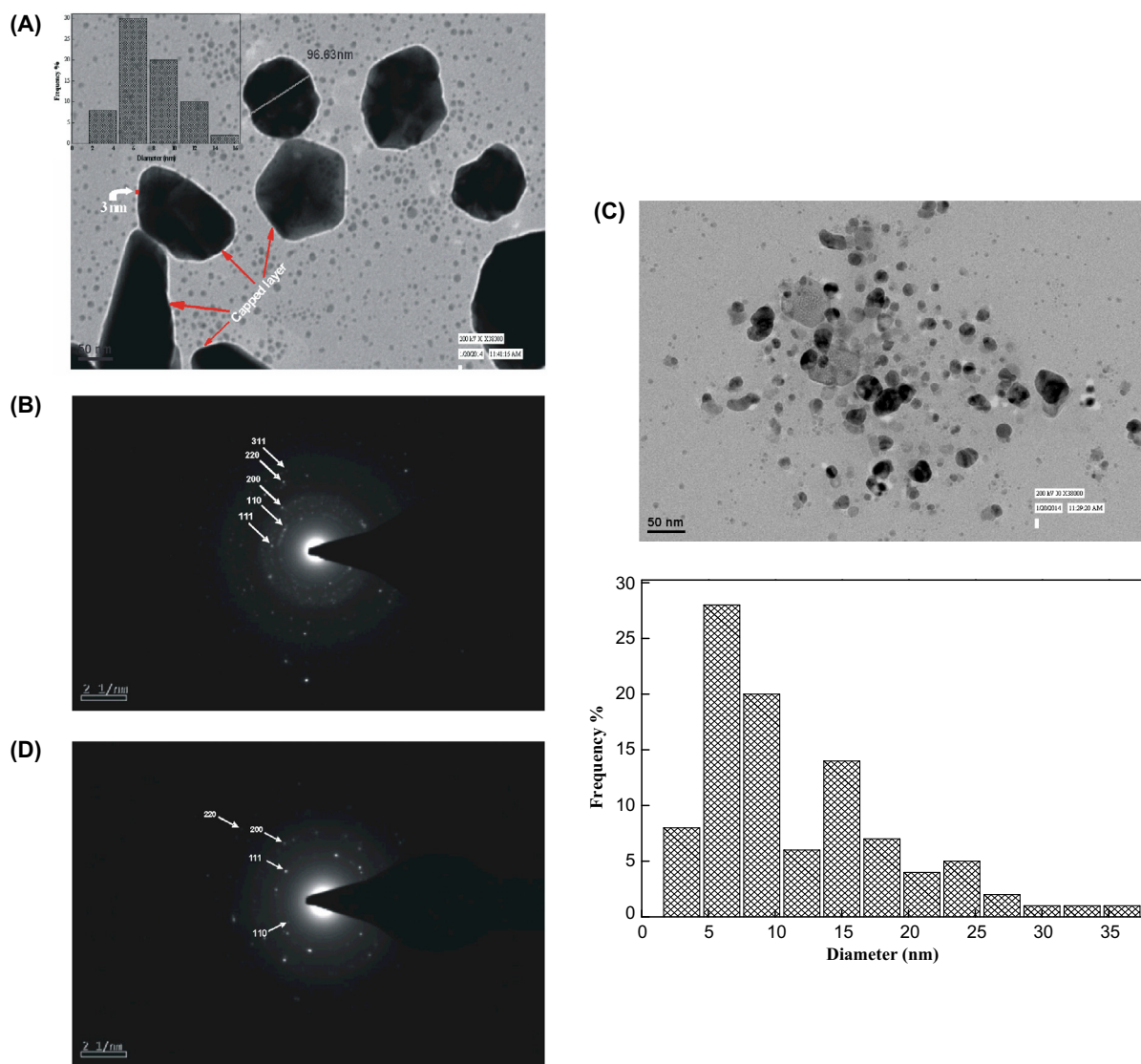


**Figure 5** TEM, size distribution histogram, and SAED images of AgNPs in absence (A and B) and presence of CTAB (C and D). Reaction conditions:  $[Ag^+] = 16.0 \times 10^{-4} \text{ mol dm}^{-3}$ ;  $[\text{extract}] = 5.0 \text{ cm}^3$ ;  $[\text{CTAB}] = 8.0 \times 10^{-4} \text{ mol dm}^{-3}$ .

$\{220\}$ ,  $\{311\}$ ,  $\{331\}$  and  $\{422\}$ , of pure face-centered cubic silver structure (Kelly et al., 2003; Serra et al., 2009). It is observed that the extract and CTAB significantly influence the morphology (size, shape and the size distribution) of AgNPs. Large numbers of quantum dots, spheres, and triangular nanoplates are produced in the presence of extracts only (Fig. 5A), while spherical and mostly irregular morphologies of different shapes are obtained in the presence of CTAB (Fig. 5C). CTAB though controls the shape and structure, cannot control the crystal growth in the subsequent steps (adsorption) resulting in anisotropic morphologies. Out of extracts and CTAB, the latter is a better capping agent because we would synthesize the truncated triangular silver nanoplates with CTAB only. These observations are in good agreement with the results of Bakshi et al. regarding the role of Gemini surfactants on the morphology of Au-nanoparticles (Bakshi et al., 2008). XRD is the main characterization method to identify whether the product was pure AgNPs. An XRD pattern at room temperature is shown in Fig. 6, confirming the

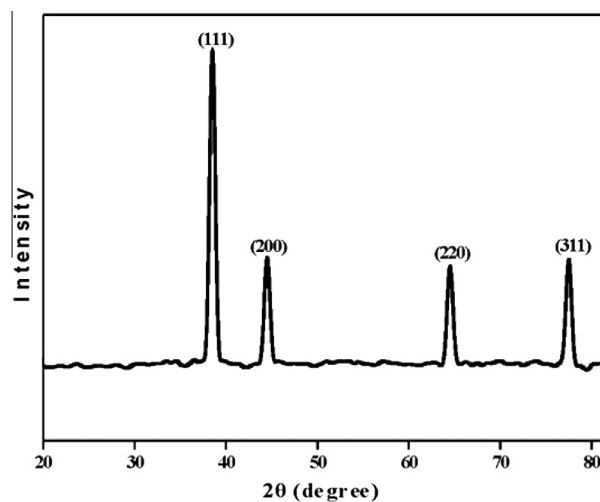


**Figure 6** XRD spectra of AgNPs. Other conditions were the same as in Fig. 5.

crystalline structure of AgNPs. The XRD peak positions are consistent with metallic silver. Bragg's reflections are observed in XRD patterns at  $2\theta$  values of 38.5, 44.5, 64.5, and 77.0, which correspond to the Miller indices of 111, 200, 220 and 311, respectively, and represent face-centered cubic (fcc) crystal structure of AgNPs. All diffraction peaks are in good agreement with the standard value (JCPDS card No. 04-0783).

#### 4. Conclusions

We reported a simple one pot chemical reduction method for the synthesis of silver nanoparticles using *oriental plane* leaf extracts with and without CTAB for the first time. The morphology, shape of the spectra and the stability of the resulting AgNPs are highly dependent on the concentration of AgNO<sub>3</sub>, leaf extracts, CTAB, pH, and reaction-time. AgNPs remain stable in the presence of high concentrations of leaf extracts. TEM images show the ring of ca. 3 nm bi-layer on the surface of the AgNPs. The present method may be helpful in the synthesis of silver nanoparticles having different morphologies by using the aqueous leaf extracts of other bioactive medicinal plants.

#### Acknowledgments

This project was funded by the Deanship of Scientific Research (DSR), King Abdulaziz University, Jeddah, under Grant no. (MS/15/301/1434). The authors, therefore, acknowledge with thanks to the DSR for technical and financial support.

#### References

- Al-Thabaiti, S.A., Al-Nowaiser, F.M., Obaid, A.Y., Al-Youbi, A.O., Khan, Z., 2008. *Colloids Surf., B* 67, 230.
- Amiri, O., Salavati-Niasari, M., Sabet, M., Ghanbari, D., 2013. *Mater. Sci. Semicond. Process.* 16, 1485.
- Amiri, O., Salavati-Niasari, M., Hosseinpour-Mashkani, S.M., Rafiei, A., Bagheri, S., 2014a. *Mater. Sci. Semicond. Process.* 27, 261.
- Amiri, O., Salavati-Niasari, M., Sabet, M., Ghanbari, D., 2014b. *Comb. Chem. High Throughput Screening* 17, 183.
- Bakshi, M.S., 2009. *Langmuir* 25, 12697.
- Bakshi, M.S., 2010. *J. Nanosci. Nanotechnol.* 10, 1757.
- Bakshi, M.S., Sachar, S., Kaur, G., Bhandari, P., Kaur, G., Biesinger, M.C., Possmayer, F., Petersen, N.O., 2008. *Cryst. Growth Des.* 8, 1713.
- Chen, S.H., Wang, Z.L., Ballato, J., Foulger, S.H., Carroll, D.L., 2003. *J. Am. Chem. Soc.* 125, 16186.
- Cierpiszewski, R., Hebrant, M., Szymanowski, J., Tondre, C., 1996. *J. Chem. Soc., Faraday Trans.* 92, 249.
- Henglein, A., 1993. *J. Phys. Chem.* 97, 5457.
- Hussain, S., Khan, Z., 2014. *Bioprocess Biosyst. Eng.* 37, 1221.
- Jin, R.C., Cho, Y.W., Markin, C.A., Kelly, K.L., Schatz, G.C., Zheng, J.G., 2001. *Science* 294, 1901.
- Kelly, K.L., Coronado, E., Zhao, L.L., Schatz, G.C., 2003. *J. Phys. Chem. B* 107, 668.
- Khan, Z., Kumar, P., Kabir-ud-Din, 2004. *Colloids Surf., A* 248, 25.
- Khan, Z., Al-Thabaiti, S.A., Obaid, A.Y., Khan, Z.A., Al-Youbi, A.O., 2012. *J. Colloid Interface Sci.* 367, 101.
- Khan, Z., Hussain, J.I., Hashmi, A.A., 2012a. *Colloids Surf., B* 95, 229.
- Khan, Z., Bashir, O., Hussain, J.I., Kumar, S., Ahmad, R., 2012b. *Colloids Surf., B* 98, 85.
- Linnert, T., Mulvaney, P., Hanglein, A., Weller, H., 1990. *J. Am. Chem. Soc.* 112, 4657.
- Mehta, S.K., Chaudhary, S., Gradzielski, M., 2010. *J. Colloid Interface Sci.* 343, 447.
- Mulvaney, P., 1996. *Langmuir* 12, 788.
- Pal, T., Sau, T.K., Jana, N.R., 1997. *Langmuir* 13, 1481.
- Pileni, M.P., 1993. *J. Phys. Chem.* 97, 6961.
- Sabet, M., Salavati-Niasari, M., Ghanbari, D., Amiri, O., Yousefi, M., 2013. *Mater. Sci. Semicond. Process.* 16, 696.
- Salavati-Niasari, M., Hosseinzadeh, G., Amiri, O., 2012. *J. Clust. Sci.* 23, 459.
- Salavati-Niasari, M., Behfard, Z., Amiri, O., Khosravifard, E., Hosseinpour-Mashkani, S.M., 2013. *J. Clust. Sci.* 24, 349.
- Serra, A., Filippo, E., Re, M., Palmisano, M., Vittori-Antisari, M., Buccolieri, A., Manno, D., 2009. *Nanotechnology* 20, 165501.
- Sharma, N.C., Sahi, S.V., Nath, S., Parsons, J.G., Gardea-Torresdey, J.L., Pal, T., 2007. *Environ. Sci. Technol.* 41, 5137.
- Shiv Shankar, S., Rai, A., Ahmad, A., Sastry, M., 2004. *J. Colloid Interf. Sci.* 275, 496.
- Song, J.Y., Kim, B.S., 2009. *Bioprocess Biosyst. Eng.* 32, 79.
- Zhang, J., Roll, D., Geddes, C.D., Lakowicz, J.R., 2004. *J. Phys. Chem. B* 108, 12210.